

RSC Advances



This is an *Accepted Manuscript*, which has been through the Royal Society of Chemistry peer review process and has been accepted for publication.

Accepted Manuscripts are published online shortly after acceptance, before technical editing, formatting and proof reading. Using this free service, authors can make their results available to the community, in citable form, before we publish the edited article. This *Accepted Manuscript* will be replaced by the edited, formatted and paginated article as soon as this is available.

You can find more information about *Accepted Manuscripts* in the [Information for Authors](#).

Please note that technical editing may introduce minor changes to the text and/or graphics, which may alter content. The journal's standard [Terms & Conditions](#) and the [Ethical guidelines](#) still apply. In no event shall the Royal Society of Chemistry be held responsible for any errors or omissions in this *Accepted Manuscript* or any consequences arising from the use of any information it contains.

LACCASE IMMOBILIZED ON PAN/O-MMT COMPOSITE NANOFIBERS SUPPORTS FOR SUBSTRATE BIOREMEDIATION: A *DE NOVO* ADSORPTION AND BIOCATALYTIC SYNERGY

Guohui Li,^a Avinav G. Nandgaonkar,^b Keyu Lu,^a Wendy E. Krause,^b Lucian A. Lucia,^{b,c,d,*} Qufu Wei^{a,*}

^a Key Laboratory of Eco-Textiles, Ministry of Education, Jiangnan University, 1800 Lihu Avenue, Wuxi, Jiangsu Province, Wuxi 214122, China

^b Fiber and Polymer Science Program, North Carolina State University, 2401 Research Drive, Campus Box 8301, Raleigh, NC 27695-8301

^c Department of Forest Biomaterials, North Carolina State University, 2820 Faucette Drive, Campus Box 8005, Raleigh, NC 27695-8005

^d Qilu University of Technology, Key Laboratory of Pulp & Paper Science and Technology of the Ministry of Education, Jinan, P.R. China 250353

Abstract: The engineering of supports for enzyme immobilization while retaining competent functionality is nontrivial. We attempted to enhance the removal efficiency of organics by adopting a relatively novel approach involving a synergy from the adsorption capabilities of a support incorporated with organically modified montmorillonite (O-MMT) and catalytic properties of immobilized laccase. Electrospun polyacrylonitrile (PAN)/O-MMT membranes after alkaline hydrolysis and carboxyl activation were chosen as the support system for laccase immobilization. Confocal laser scanning microscope confirmed a uniform enzyme distribution along with the fibers' longitudinal surface. After enzyme immobilization, the optimum pH shifted from 3 to 3.5, while the optimum temperature remain unchanged at 50 °C. Its stability was preserved despite a large fluctuation in pH (50% of its initial activity retained over the pH range 2-6) and temperature (more than 80% of its initial activity retained over 30-70 °C). Compared to free laccase, the thermal stability of the immobilized laccase

28 was improved after being under 30 °C and 50 °C for 8 h. The operational stability was 68%
29 of its initial after 10 times repeated usage, while also demonstrating 80% storage stability of
30 initial activity even after two months. The immobilized laccase showed high removal
31 efficiency of crystal violet at an optimum pH of 5 and temperature ~ 40 °C as well as an
32 initial substrate concentration of 100 mg/L. Compared with that of individual support and the
33 free laccase, the removal efficiency by immobilized enzyme is far higher to confirm a
34 synergy in the immobilized enzyme and support system.

35

36 **Keywords:** *Biocatalysis, Adsorption, Enzyme Immobilization, Electrospinning, Composite*
37 *Nanofibers*

38

39 Introduction

40 Triphenylmethane dyes (TPM) are synthetic colorants extensively used in paper, leather,
41 and pharmaceuticals, but predominantly within the textile industries.¹ Approximately
42 thousands of tons of textiles dyes end up in receiving waters due to improper processing and
43 dyeing technologies and thereby causing contamination. Among the many types of dyes,
44 crystal violet (CV) results in 10-15% of unused dye released into the environment per annum
45 ² which not only compromises water quality, but degrades the aesthetic value of water
46 ecosystems. TPM dyes are recalcitrant to degradation due to their complex structure and
47 aromatic rings while additionally being carcinogenic, toxic, and mutagenic.^{3,4} Crystal violet
48 (CV) is also known to cause permanent injury to corneas, skin irritation, kidney failure, and
49 permanent blindness after adventitious poisoning of drinking water systems.⁵

50 Several physical and chemical methods, such as flocculation, coagulation, adsorption,
51 membrane filtration and ozonation have been applied to treat wastewater containing colored
52 effluents. However, the main drawbacks has been high cost, inability to totally remove
53 recalcitrant dyes, and also an apparent production of large amounts of sludge which restrict
54 their applications.^{6,7} Recently, the paradigm of enzyme-based bioremediation for
55 contaminated waste water has been gaining ascendancy over many other approaches because
56 of superior physical and chemical operational parameters that include mild treatment
57 conditions, high efficiency, low cost, and its competency to treat large effluent volumes.⁸ In
58 one prototypical approach, laccase (polyphenoloxidase, EC 1.10.3.2), a multi-copper enzyme,
59 has been shown to oxidize a variety of organic substrates. The process of laccase-based
60 catalysis only requires the presence of the substrate and O₂ as the terminal oxidant to display

61 optimal behavior in decontamination schemes.⁹

62 Free laccase has certain limitations, such as low stability, recyclability, and reusability in
63 industrial applications which has then led to the suggestion of a possible solution by enzyme
64 immobilization,^{10,11} which has been shown to significantly improve long-term enzymatic
65 reactivity, stability, and efficiency even under harsh conditions, but the quest for appropriate
66 supports is ongoing.¹²⁻¹⁴ Zhang et. al¹⁵ vividly identified bottlenecks for laccase-based
67 catalysis in potential secondary pollution by-products. Thus, if the carrier can also work as
68 an adsorbent for potential pollution by-products, it could effectively solve the issue
69 mentioned herein.

70 Among immobilizing carriers, electrospun fibrous membranes possessing mesoporous
71 structures have shown great potential because of their large surface area, inter-fiber porosity,
72 fiber diameters from several micrometers to nanometers, and good mechanical strength.
73 These properties ensure enhanced enzyme loading, recycling, and reuse. An additional benefit
74 can be achieved through cross-linking for enzyme immobilization to ensure stabilization and
75 prevention of leaching in larger mesoporous membranes.¹⁶

76 In particular, electrospinning has proven useful to produce polymeric nanofibers
77 membranes for absorbing contaminants. Among these polymeric nanofibers, PAN has been
78 widely used for filtration and adsorption because of its good mechanical strength and
79 stability.¹⁷ Xu et al.¹² designed a mesoporous membrane (pore size 1.73-3.54 nm, pore
80 volume 0.379 cm³/g, and specific surface area = 542.91 m²/g) by extracting hexadecyl
81 trimethyl ammonium bromide (CTAB) from electrospun PAN nanofibers followed by laccase
82 immobilization as a means to target *Triclosan*, a ubiquitous antibacterial/antifungal consumer

product. Remarkably, it was demonstrated that a combination of adsorption and degradation was indeed effective. In fact, the previous work in this lab demonstrated that an adsorption/enzyme catalysis-combined strategy¹³ demonstrates great value: PAN/organically-modified montmorillonite (PAN/O-MMT) electrospun composite nanofibrous membranes for laccase immobilization can be successfully prepared and demonstrated. However, that specific effort focused on system applications; thus, industrial-grade laccase and a rudimentary adsorption process were used for enzyme immobilization. Nevertheless, a mechanistic basis for its activity was not explored because the enzyme system was impure and displayed inherent instability, which is important in understanding the synergic mechanism; hence, making it possible to provide satisfactory results.

Thus, the current work examined an immobilized, highly pure laccase system covalently attached to the surface of electrospun PAN nanofibers within which O-MMT was incorporated as a versatile adsorbent and distributing agent. This study reveals that crystal violet (CV) can be effectively bio-remediated using a combined adsorption/biocatalysis process. The kinetic, stability, and physical properties of the immobilized laccase were studied and CV bio-remediation factors influenced by immobilized laccase were also investigated.

101

102 **Experimental**

103 Materials

104 Laccase from *Trametes versicolor* was purchased from Sigma-Aldrich. 2,

2'-Azino-bis(3-ethylbenzothiazoline-6-sulfonic acid) diammonium salt (ABTS), used as the substrate to determine enzyme activity, was obtained from Richu Biosciences Co. Ltd (Shanghai, China). 1-ethyl-3-(3-dimethylamino-propyl) carbodiimide (EDC) and N-hydroxysuccinimide (NHS) were purchased from Aladdin. Organically modified montmorillonite (O-MMT, modified by CTAB) was provided by Zhejiang Fenghong New Material Co., Ltd (Zhejiang, China). Polyacrylonitrile (PAN) ($M_w=50000 \text{ g mol}^{-1}$) powders were purchased from Shangyu Wu & Yue Economic and Trade Co., Ltd (Zhejiang, China). All other reagents including crystal violet (CV), sodium hydroxide (NaOH), and N,N-dimethyl formamide (DMF) were purchased from Sinopharm Chemical Reagent Co., China. Deionized water was the solvent of choice in the study.

Preparation of PAN/O-MMT composite nanofibers by electrospinning

Electrospun PAN/O-MMT composite nanofibers were fabricated as follows: first, 0.15 g O-MMT powder was well dispersed in 20 mL DMF solution by sonication for 1 h followed by the addition of 3 g PAN powder into the slurry. It was magnetically stirred for 8 hrs until a light yellow transparent solution was obtained. The as-prepared electrospinning solution was poured into a 20 mL plastic syringe equipped with a stainless steel needle that was connected to a high-voltage generator. The applied voltage was set to 15 kV while a flow rate of 0.5 mL/h was maintained. The distance between the needle tip to the collector was 15 cm.

Chemical modification of PAN/O-MMT composite nanofibers

The as-electrospun nanofibrous membranes were chemically modified as follows: a relatively uniform area of the PAN/O-MMT composite nanofibrous membrane was cut into a circular shape at a diameter of 9 cm. A 200 mL blend solution of absolute ethanol and

deionized water with a volume ratio of 19:1 was prepared, into which 8 g NaOH was added. The solution was transferred into a round-bottom flask after full dissolution of the NaOH. The membrane was placed into the flask and allowed to react at 85 °C for 20 min. The alkaline modified membrane was thoroughly washed until neutral pH was obtained. An alkaline-hydrolyzed PAN/O-MMT composite nanofibrous membrane was obtained.

EDC and NHS were used to activate the carboxyl group of the alkaline-modified PAN nanofibrous membranes using the protocol proposed in Kim's work¹⁸ with slight modifications. A detailed process is briefly described as follows: first, the alkaline modified PAN membrane was immersed in a phosphate buffer saline (PBS) buffer solution (pH=6.5) for 20 min to remove impurities. The membrane was removed and immersed in an EDC/NHS buffer solution (the molar ratio of EDC·HCl/NHS=1:1) for 3 hrs at room temperature. The membrane was then removed and washed repeatedly.

Laccase immobilization

The activated PAN/O-MMT composite nanofibrous membrane was added into 100 mL of laccase solution (0.3 g/L, pH=4) and cross-linked for 3 h in a shaking bath at 25 °C. Afterward, the membranes were taken out and washed thoroughly with buffer solution until no enzyme was detected in the washing solution. The quantity of the immobilized laccase was calculated according to Bradford's method.¹⁹ Later, the nanofibrous membrane with immobilized laccase was stored at 4 °C for further use.

Physicochemical characterization of the PAN/O-MMT nanofibrous membrane

Scanning electron microscope (SEM, Quanta 200, Holland FEI Company) was used to investigate the effect of alkali hydrolysis and carboxyl activation on the fibrous structure of

the PAN/O-MMT composite nanofibers. The samples were coated with a thin layer of gold by sputtering before the SEM imaging.

The immobilized enzyme on the surface of PAN/O-MMT composite nanofibrous membrane was labeled by an fluorescein isothiocyanate (FITC) aqueous solution and washed thoroughly by buffer solution before analysis. The membrane was carefully placed on a glass slide to which one drop of water was applied to fully unfold the membrane. A cover slip was applied to seal the membrane. Confocal laser scanning microscope (CLSM, TCS SP8) was used to characterize the immobilized enzyme at an excitation wavelength of 488 nm.

The functional groups of the PAN/O-MMT nanofibers before and after chemical treatment as well as the laccase immobilized nanofibers were obtained with Fourier Transform Infra-Red attenuated total reflectance (FTIR-ATR, Nicolet Nexus, Thermo Electron Corporation) equipped with a germanium crystal. The spectra were recorded after 16 scans at a resolution of 4 cm⁻¹.

Determination of enzyme activity

The activity of the free and immobilized laccase was assayed at 30 °C using ABTS as the substrate. A detailed process was previously reported.²⁰ Specifically, 15 mM of an ABTS solution was prepared by delivering 82.305 mg of ABTS to 10 ml of deionized water in a centrifuge tube. The activity of free and immobilized laccase was determined according to established assay protocols. In brief, the reaction assay consisted of 0.1 mM ABTS, 100 mM sodium acetate buffer (pH = 4.5) and a suitable amount of free and immobilized laccase. The assay was run by adding 0.1 mL ABTS (15 mM) into 2.9 mL sodium acetate buffer

containing a specific amount of free or immobilized laccase after which the absorbance was monitored by UV-1700 spectrophotometry at a maximum absorbance wavelength of 420 nm. For the immobilized laccase, the sample was centrifuged at 12,000 rpm for 40 sec, and the supernatant was used for monitoring the laccase activity. All assays were conducted in triplicate at minimum.

Kinetic studies

Kinetics studies were carried out at 30 °C in 100 mM sodium acetate (pH=4.5) buffer using ABTS as the substrate having the substrate concentration varying from 0.1 to 1 mM. The kinetic parameters of K_m and V_{max} were calculated according to the Lineweaver-Burk double reciprocal models using Equation (1).²¹

$$1/v = (K_m/V_{max})(1/S) + 1/V_{max} \quad (1)$$

Optimum pH and temperature

To determine the optimum pH, the immobilized enzymes were incubated in buffers at pHs ranging from 2 to 6 at 4 °C for 12 h and assayed for activity, while the optimum temperature was determined by the activities of the immobilized enzymes incubated in buffers (pH 4.5) at 10 min over different temperatures ranging from 30 to 70 °C before adding ABTS.

Stability of free and immobilized laccase

The thermal stability of free and immobilized laccase was evaluated by the relative activity at 30°C and 50 °C recorded at 2 h intervals. The experiments were conducted in 100 mM buffer solutions at pH 4.5.

The operational stability was studied by repeated usage (10 ×), while the relative enzyme activity was recorded after each use. The experiments were carried out at 30 °C and pH 4.5.

193 All the control samples were made with the buffer solution at the same pH value as the
194 assayed sample.

195 The storage stability of the immobilized enzyme was determined by the activity retention
196 ratio during storage at 4 °C in 100 mM sodium acetate buffer solution (pH 4.5) at regular
197 intervals up to 60 days.

198

199 Removal of CV

200 Effect of initial concentrations (10, 25, 50, 100, 150 mg/L), pH (2-6) and temperature
201 (20-70 °C) on the removal efficiency of CV was determined using a UV-1700
202 spectrophotometer at a wavelength of 590 nm.

203 All assays were conducted in triplicate at minimum. Experimental data were reported as
204 mean \pm standard deviation. Statistical differences were analyzed using one-way ANOVA
205 whiles statistical significance was represented as $p < 0.05$.

206

207 **Results & Discussion**

208 Morphology and structural transformation after chemical modification and enzyme 209 immobilization

210 SEM images as well as their corresponding digital photographs are shown in Figure 1
211 (a-c) to evaluate the morphological and structural changes that were induced subsequent to
212 alkaline hydrolysis and carboxyl activation.

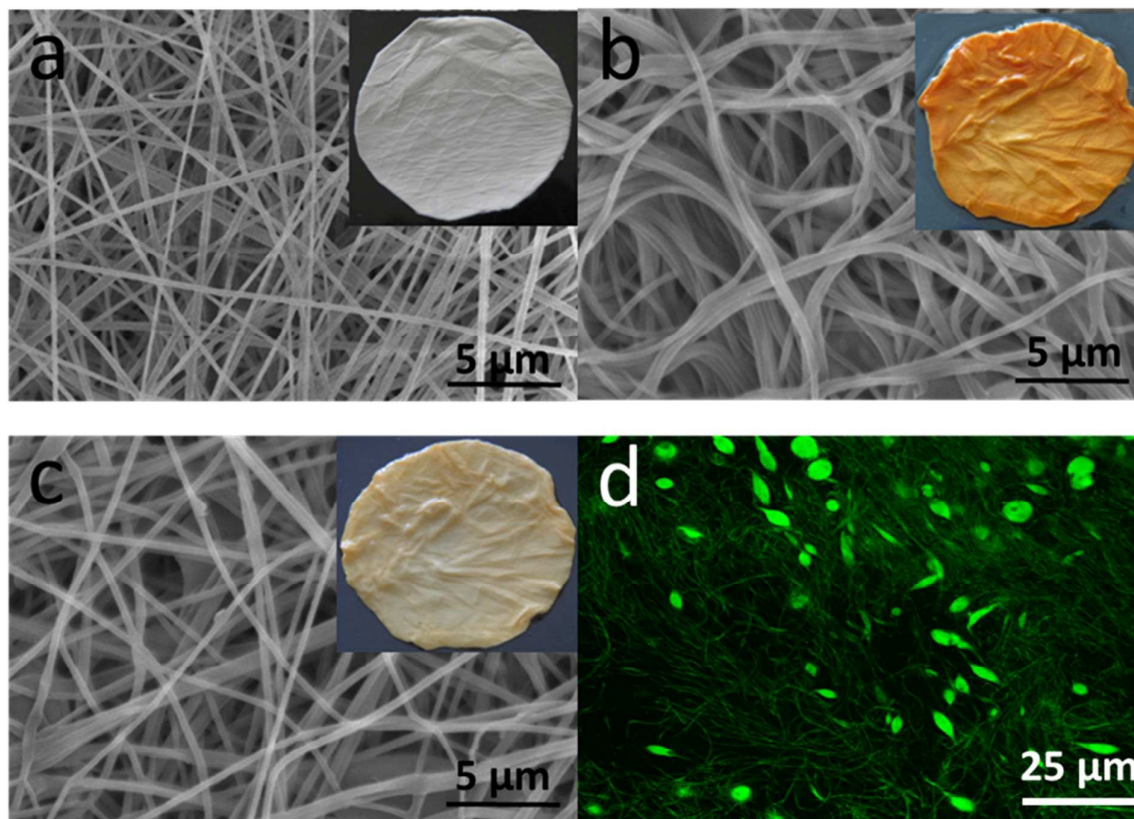


Figure 1. SEM and digital photographs of PAN/O-MMT composite nanofibers before and after chemical modification: (a) PAN/O-MMT composite nanofibrous membrane; (b) PAN/O-MMT composite nanofibrous membrane after alkaline hydrolysis; (c) PAN/O-MMT composite nanofibrous membrane after carboxyl activation. (d) Confocal Laser Scanning Microscope (CLSM) photo-micrographs of PAN/O-MMT composite nanofibrous membranes after enzyme immobilization.

It was noted that the color of the PAN/O-MMT composite nanofibrous membranes ostensibly changed after chemical modification. Indeed, the alkaline hydrolysis produced a brownish yellow membrane that notably possessed much superior mechanical properties. The color change likely originated from intermediates that have poly-conjugated character generated from electrocyclization in the early hydrolysis stage.²²⁻²⁴ During this period of incubation, carboxyl and amide groups were formed that not only provide active sites for

enzyme immobilization, but also gave rise to mechanical strength from a combination of hydrogen bonding effects. The ensuing EDC/NHS modification step for carboxyl activation changed the membrane color from brown-yellow to light yellow that is likely due to a chemical transformation/consumption of unstable intermediates.

It can be also noted from Figure 1 (a-c) that apart from the color changes, the fibrous microstructure also significantly changed. The original PAN/O-MMT composite nanofibers displayed good morphology with a diameter distribution over 200-300 nm (Fig. 1a). After alkaline hydrolysis, it was observed that the nanofibers assumed tortuous entanglements amongst one another in which adjacent nanofibers adhered to each other (Fig. 1b). This is likely induced by a chemical and physical “refining” arising from the hydrolytic action of OH^- at high temperatures. After EDC/NHS activation of the carboxyl group (Fig. 1c), it was observed that the fibers appeared to decouple as if they were relaxing to their original state. Specifically, the fibers generally repelled and redistributed individually.

Figure 1d illustrates a CLSM photo-image of PAN/O-MMT composite nanofibers containing the immobilized laccase. The FITC-labeled (green) laccase can be observed to be more or less uniformly distributed throughout the nanofiber network. This CLSM image also verifies that enzyme molecules have been successfully immobilized onto the surfaces of the solid support.

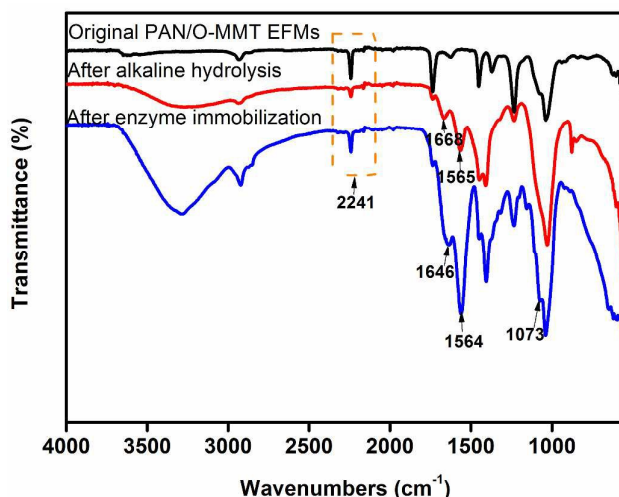


Figure 2. FTIR spectra of PAN/O-MMT composite nanofibers before and after alkaline hydrolysis and enzyme immobilization.

The chemical structure of PAN nanofibers was changed after alkaline hydrolysis and enzyme immobilization as confirmed by FT-IR presented in Figure 2. The original PAN nanofibers show a peak at 2241 cm^{-1} for the nitrile group ($-\text{CN}$) and 1628 cm^{-1} for the low level of vinyl groups ($-\text{C}=\text{CH}-$).²² The hydrolysis leads to the development of two new peaks at 1565 cm^{-1} and 1668 cm^{-1} , respectively, indicating the presence of $-\text{COONa}$ and $-\text{CONH}_2$ groups in the modified fiber.²⁵ After enzyme immobilization, the FTIR spectrum of laccase-PAN nanofibers showed two peaks at 1564 and 1646 cm^{-1} , which can be attributed to amide I (the vibration of the $\text{C}=\text{O}$ bonds) and amide II (a combination of $\text{C}-\text{N}$ stretching and $\text{N}-\text{H}$ vibration in protein backbone), respectively.^{8, 26} Meanwhile, a new peak at 1073 cm^{-1} appears, representing $\text{C}-\text{N}$ bonds formed between the enzyme and PAN after laccase immobilization.⁸ This observation confirms the assertion that laccase is covalently immobilized onto the surface of PAN nanofibers.

Catalytic activity of free and immobilized laccase

Table 1. Kinetic parameters of the immobilized laccase.

	Enzyme loading (mg/g nanofiber)	Retention activity (%)	K_m (μM)	V_{max} ($\mu\text{mol/mg min}$)
Free Laccase	-		120.32	595.24
Immobilized Laccase	276	73.5	622.15	293.46

261

262

263 The amount of enzyme loading and kinetic parameters K_m and V_{max} are shown in Table 1.

264 The enzyme loading is 276 mg per gram of support, a value that is higher than reported by

265 Ran Xu (220 mg/g) ⁸ whose work also used PAN nanofibrous membrane after chemical

266 modification for laccase immobilization. The relative activity of the immobilized laccase was

267 73.5%, which is slightly higher than the laccase immobilized onto the amide-modified PAN

268 nanofibers (72% of its specific activity).

269 The K_m value of the immobilized laccase was much higher than that of free laccase while

270 the V_{max} value was significantly decreased. The difference between K_m and V_{max} after

271 immobilization may be due to a lower accessibility between the substrate and active points of

272 the immobilized enzyme because of higher diffusion limitations that arise from the space

273 barriers of the support that result in a lower probability of forming an enzyme-substrate

274 complex. ⁸

275 Optimum pH and temperature

276 Studies on the optimum pH and temperature for our system give information on suitable

277 conditions for the enzymatic activity. Figure 4 shows the optimum pH and temperature of

278 both free and immobilized laccase. The variation of pH has a pronounced effect on the

279 enzyme stability likely from two reasons: first, a change in pH can denature the enzyme,

280 while secondly, pH can influence the dissociation of enzyme active sites; hence, restricting
281 reaction with the substrate.²⁷ A pH range of 2-6 was therefore selected over which the
282 enzyme activity could be evaluated.

283 The optimum pH for free laccase was 3, whereas that of immobilized laccase shifted to 3.5
284 (Fig. 3a). The same results were also observed in previous work with PAN/O-MMT in
285 which it was used as a support for immobilized laccase via an adsorption method.¹³ The basis
286 for the observed results is that MMT intercalated within the PAN polymer matrix and was
287 able to adsorb H^+ from the buffer solution; thus, it was able to make the surface of the support
288 more acidic than the buffer solution. Not surprisingly, the immobilized laccase demonstrated
289 a higher activity over relatively higher pH. In addition, bound laccase could significantly
290 broaden the operational pH range.

291 The optimum temperature for both free and immobilized laccase was 50 °C (Fig. 3b). In
292 general, for free laccase, reduced or elevated temperature has a significant dampening effect
293 on its activity in direct opposition to what we observed for the immobilized laccase. Over
294 30-70 °C, the variation of the enzyme activity was very small; even at 70 °C, it still retained
295 more than 80% of its activity. Immobilization therefore can significantly improve enzyme
296 activity despite fluctuations in temperature because of the presence of multi-linkages among
297 nanofibers over which the enzyme molecules can maintain a stable conformation, thus
298 preventing compromise of enzyme function.

299

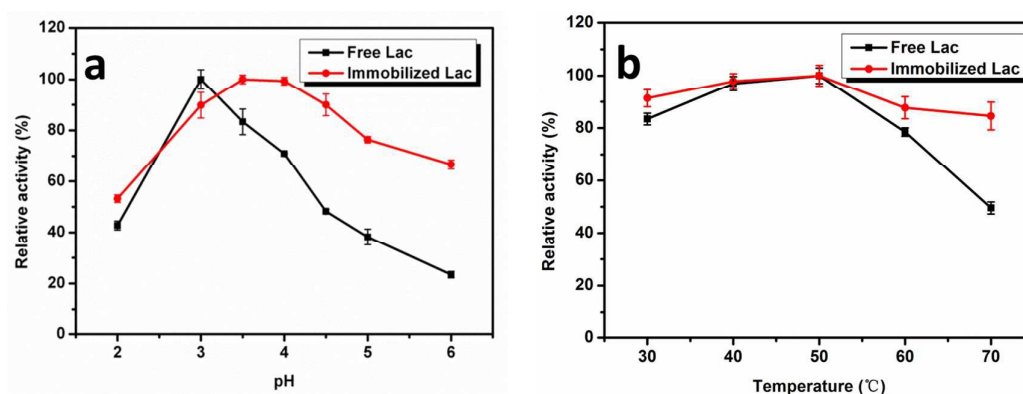


Figure 3. Effects of pH (a) and temperature (b) on laccase activity.

Thermal stability

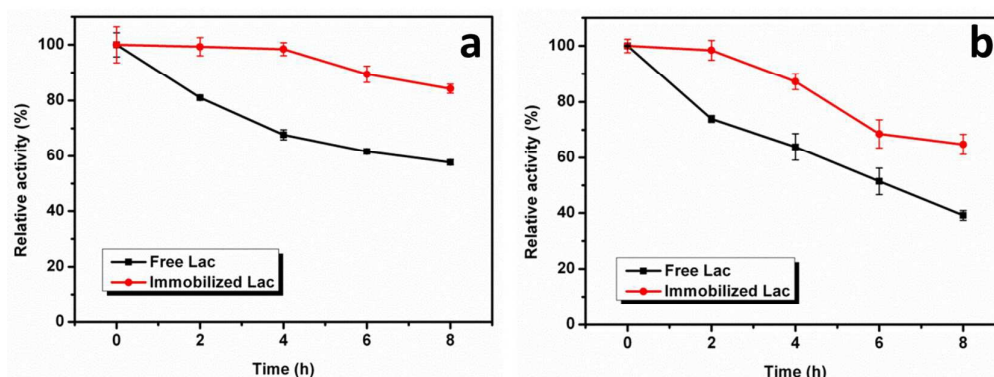


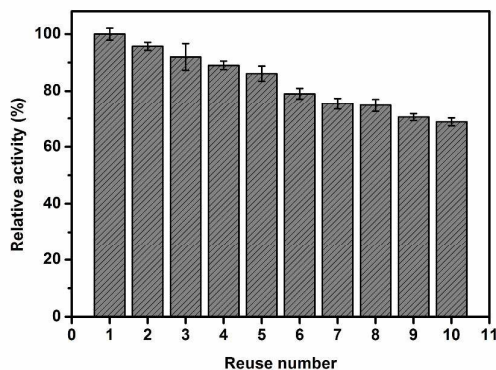
Figure 4. Thermal stability of free and immobilized laccase at (a) 30 °C and (b) 50 °C.

The thermal stability was studied at 30 °C and 50 °C and recorded every 2 h. The initial enzyme activity was set as 100%, while the relative enzyme activity at different time intervals was calculated; all results are shown in Figure 4.

At a lower temperature, both free and immobilized laccase showed better thermal stability than at higher temperatures. At 30 °C after 8 h, the free laccase retained 57 % of its initial activity, while the immobilized laccase maintained 85 % (Fig.4a). At 50 °C (8 h), the activity for both free and immobilized laccase were approximately 38 % and 66 %, respectively.

314 respectively (Fig.4b). The results indicated a more preferable thermal stable laccase after
 315 immobilization. The improvement in resistance over temperature was probably due to a
 316 reduction in molecular mobility and conformational changes because of the immobilization
 317 on PAN/O-MMT composite nanofibers supports.²⁸

318 Operational stability



319
 320 **Figure 5.** Reusability of the immobilized laccase.

321
 322 Reusability is one of the most important aspects for immobilized laccase.²⁹ Figure 5 shows
 323 the operational stability at room temperature. After 5 cycles, it retained nearly 85 % of its
 324 initial activity. Additionally, about 70 % of the initial activity were retained after 10 cycles.
 325 The results shown indicate good reusability of the laccase immobilized on PAN/O-MMT
 326 composite nanofibers. This work showed better reusability that was able to maintain 70% of
 327 the initial activity after 10 cycles compared with other immobilization methods,^{28,13} whereas
 328 the reusability property of immobilized is essential for cost-effective use of the enzyme in
 329 biotechnological applications.

Storage stability

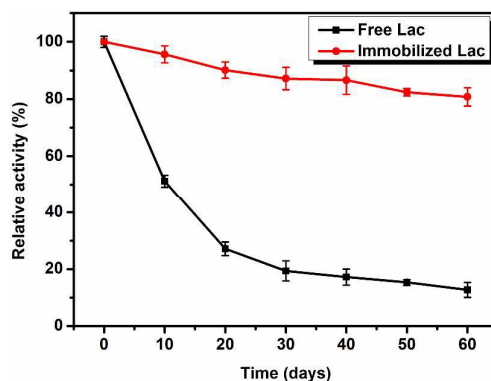


Figure 6. Storage stability of free and immobilized laccase at 4 °C.

Figure 6 illustrates the storage stabilities of free and immobilized laccase in aqueous solution. Free laccase showed continuous inactivation, while immobilized laccase exhibited negligible activity loss over two month. This result suggests that the multi-point covalent linkages for the laccase molecules effectively prevented the enzymes from being denatured and/or leaching.³⁰

The effect of initial concentration of CV on its removal

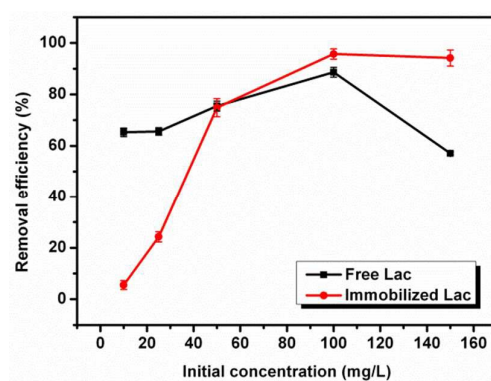


Figure 7. Effect of initial concentration on CV removal efficiency.

Figure 7 shows the effect of initial concentration of CV on removal efficiency. As the

initial concentration increased from 10 to 100 mg/L, the removal efficiency of CV by both free and immobilized laccase increased. However, when the concentration increased to 150 mg/L, the removal efficiency decreased. Due to diffusional limitations, immobilized laccase showed very low capacity in removing CV from aqueous solution when it was at low concentration.

The effect of pH value and temperature on dye removal efficiency

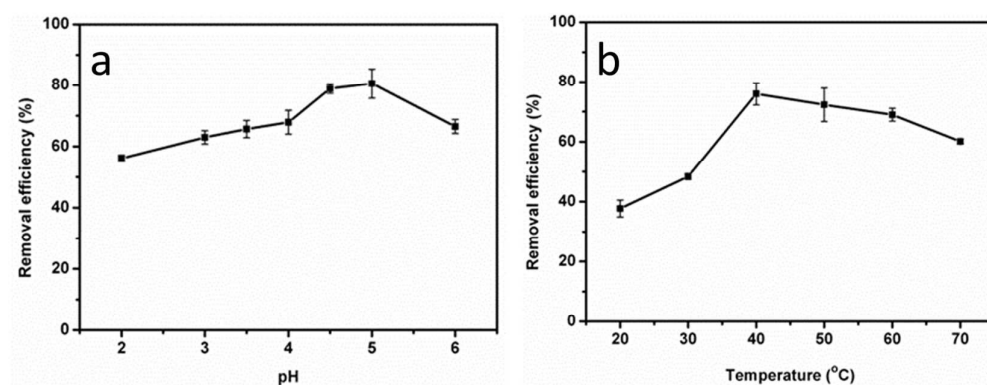


Figure 8. The effect of pH value (a) and temperature (b) on dye removal efficiency.

Variation of pH and temperature also affected dye degradation. The results of the removal efficiency of CV under different pH and temperature are shown in Figure 8.

When the pH increased from 2 to 5, CV removal efficiency increased; when pH further increased, the CV removal efficiency decreased (Figure 8a). As is well known, large quantities of H^+ in buffer solution compete with CV for adsorption sites on O-MMT. Thus, when the buffer solution becomes less acidic, the adsorption of CV is more efficient. However, when $pH \sim 6$, the laccase showed very low catalytic capacity, thus reducing the overall removal efficiency. This finding was consistent with that of Xu et al.³¹

The optimum temperature for CV adsorption is 40 °C. It was revealed that higher

temperatures can assist CV molecules diffusion into the fiber matrix and improve adsorption; but when the temperature was further increased, laccase became partially denatured, thus decreasing the degradation efficiency. The results were similar to previous findings, possibly due to the common denaturing observed as a result of unfavorable conditions.³¹

The effect of time on dye removal efficiency

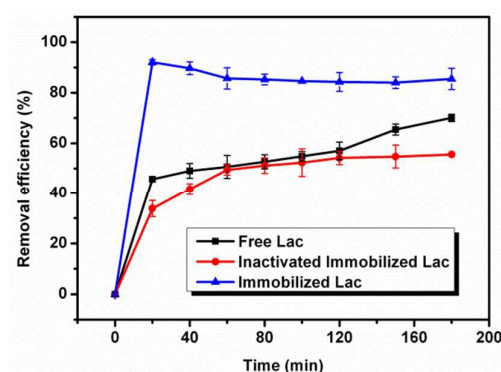


Figure 9. The effect of the free laccase (Lac), immobilized laccase, and the support on dye removal efficiency.

Figure 9 shows the removal efficiency of CV in a 3 h batch experiment. The total degradation of CV by free laccase was ~ 70 % over 3 h, while the adsorption ratio of CV by the support itself was 50 %. The removal efficiency of immobilized laccase is ~ 91 %, a value much higher than the degradation efficiency or adsorption effect itself, achieving equilibrium within 20 min, where the removal efficiency is higher than the total effect of both free laccase (45 %) and support (33 %). The result suggested a synergistic effect between the support itself and immobilized laccase. The synergistic removal efficiency was higher than the grapefruit peel,³² which adsorbed ~ 60% CV within 20 min and required 90 min to achieve 90% removal.

Conclusions

Electrospun PAN/O-MMT composite nanofibrous membranes after alkaline hydrolysis and carboxyl activation were successfully used as a support system to covalently immobilize laccase. CLSM confirmed that the surface of PAN/O-MMT composite nanofibrous membrane was uniformly coated with FITC-labeled laccase at a loading as high as 276 mg/g of nanofibrous membrane. Compared with free laccase, the stability of immobilized laccase was significantly improved despite significant fluxes in pH, elevated temperature, repeated usage, and extended storage. The removal of CV showed a synergistic effect between O-MMT and laccase, resulting in 91% of CV removal within 20 min. These results indicate that laccase immobilized on functional nanofibers demonstrates an attractive potential for remediating organic substrates in industrial waters, especially by the tandem adsorption and degradation phenomena that behaves in a remarkably efficient manner, and thus decrease the cost and encourage industrial applications.

Acknowledgments

This work was financially supported by the Fundamental Research Funds for Doctoral Graduates (No. KYLX_1137) and the Fundamental Research Funds for the Central Universities (JUSRP115A04). We also acknowledge the platform of the International Joint Research Laboratory for Advanced Functional Textile Materials at Jiangnan University.

References

- 1 N. Daneshvar, M. Ayazloo, A.R. Khataee and M. Pourhassan, *Bioresource Technol.*, 2007, **98**, 1176-1182.
- 2 U. Shedbalkar, R. Dhanve and J. Jadhav, *J. Hazard. Mater.*, 2008, **157**, 472-479.
- 3 T. Robinson, G. McMullan, R. Marchant and P. Nigam, *Bioresource Technol.*, 2001, **77**, 247-255.
- 4 J.P. Jadhav and S.P. Govindwar, *Yeast*, 2006, **23**, 315-323.
- 5 J.J. Jones and J.O. Falkinham, *Antimicrob. Agents Ch.*, 2003, **47**, 2323-2326.
- 6 E. Franciscon, F. Piubeli, F. Fantinatti-Garboggini, C.R. de Menezes, I.S. Silva, A. Cavaco-Paulo, M.J. Grossman and L.R. Durrant, *Enzyme Microb. Tech.*, 2010, **46**, 360-365.
- 7 A.R. Khataee, M.N. Pons and O. Zahraa, *J. Hazard. Mater.*, 2009, **168**, 451-457.
- 8 R. Xu, C.L. Chi, F.T. Li and B.R. Zhang, *Acs Appl. Mater. Inter.*, 2013, **5**, 12554-12560.
- 9 T. Kudanga and M. Le Roes-Hill, *Appl. Microbiol. Biot.*, 2014, **98**, 6525-6542.
- 10 M. Asgher, M. Shahid, S. Kamal and H.M.N. Iqbal, *J. Mol. Catal. B-Enzym.*, 2014, **101**, 56-66.
- 11 M. Fernandez-Fernandez, M.A. Sanroman and D. Moldes, *Biotechnol. Adv.*, 2013, **31**, 1808-1825.
- 12 R. Xu, Y.F. Si, X.T. Wu, F.T. Li and B.R. Zhang, *Chem. Eng. J.*, 2014, **255**, 63-70.
- 13 Q.Q. Wang, J. Cui, G.H. Li, J.N. Zhang, D.W. Li, F.L. Huang and Q.F. Wei, *Molecules*, 2014, **19**, 3376-3388.
- 14 J.W. Hou, G.X. Dong, Y. Ye and V. Chen, *J. Membrane Sci.*, 2014, **452**, 229-240.
- 15 X.L. Zhang, B.C. Pan, B. Wu, W.M. Zhang and L. Lu, *Bioresource Technol.*, 2014, **164**, 248-253.
- 16 M.R. El-Aassar, *J. Mol. Catal. B-Enzym.*, 2013, **85-86**, 140-148.
- 17 D. Selloum, A. Abou Chaaya, M. Bechelany, V. Rouessac, P. Miele and S. Tingry, *J. Mater. Chem. A*, 2014, **2**, 2794-2800.
- 18 B.C. Kim, X.Y. Zhao, H.K. Ahn, J.H. Kim, H.J. Lee, K.W. Kim, S. Nair, E. Hsiao, H.F. Jia, M.K. Oh, B.I. Sang, B.S. Kim, S.H. Kim, Y. Kwon, S. Ha, M.B. Gu, P. Wang and J. Kim, *Biosens. Bioelectron.*, 2011, **26**, 1980-1986.

- 428 19 M.M. Bradford, *Anal. Biochem.*, 1976, **72**, 248-254.
- 429 20 Q.Q. Wang, L. Peng, Y.Z. Du, J. Xu, Y.B. Cai, Q. Feng, F.L. Huang and Q.F. Wei, *J.*
430 *Porous. Mat.*, 2013, **20**, 457-464.
- 431 21 K. Ward, J. Xi and D.C. Stuckey, *Biotechnol. Bioeng.*, 2015, **9999**, 1-9.
- 432 22 K.I. Lee, J.H. Li, B. Fei and J.H. Xin, *Polym. Degrad. Stabil.*, 2014, **105**, 80-85.
- 433 23 I.V. Ermakov, A.I. Rebrov, A.D. Litmanovich and N.A. Plate, *Macromol. Chem. Physic.*,
434 2000, **201**, 1415-1418.
- 435 24 A.D. Litmanovich and N.A. Plate, *Macromol. Chem. Physic.*, 2000, **201**, 2176-2180.
- 436 25 M.L. Gupta, B. Gupta, W. Oppermann and G. Hardtmann, *J. Appl. Polym. Sci.*, 2004, **91**,
437 3127-3133.
- 438 26 P. Sathishkumar, S. Kamala-Kannan, M. Cho, J.S. Kim, T. Hadibarata, M.R. Salim and
439 B.T. Oh, *J. Mol. Catal. B-Enzym.*, 2014, **100**, 111-120.
- 440 27 A. Kumari and A.M. Kayastha, *J. Mol. Catal. B-Enzym.*, 2011, **69**, 8-14.
- 441 28 J.P. Hu, B.N. Yuan, Y.M. Zhang and M.H. Guo, *Rsc Adv.*, 2015, **5**, 99439-99447.
- 442 29 F. Quintanilla-Guerrero, M.A. Duarte-Vazquez, B.E. Garcia-Almendarez, R. Tinoco, R.
443 Vazquez-Duhalt and C. Regalado, *Bioresource Technol.*, 2008, **99**, 8605-8611.
- 444 30 J.J. Roy and T.E. Abraham, *Chem. Rev.*, 2004, **104**, 3705-3721.
- 445 31 R. Xu, Q.J. Zhou, F.T. Li and B.R. Zhang, *Chem. Eng. J.*, 2013, **222**, 321-329.
- 446 32 A. Saeed, M. Sharif and M. Iqbal, *J.Hazard. Mater.*, 2010, **179**, 564-572.

Graphical Abstract

